






INVESTIGATING THE EFFECTS OF CRACK ORIENTATION AND DEFECTS ON PIPELINE FATIGUE LIFE THROUGH FINITE ELEMENT ANALYSIS

Tayeb Kebir^{1,2,*}, Mohamed Belhamiani³, Ahmed Amine Daikh^{1,4},
Mohamed Benguediab² and Mustapha Benachour⁵

¹ Artificial Intelligence Laboratory for Mechanical and Civil Structures and Soil,
Department of Mechanical Engineering, Institute of Technology, University Center of
Naama, Naama 45000, Algeria.

² Laboratory of Materials and Reactive Systems, University of Sidi Bel Abbes, Algeria.

³ Smart Structures Laboratory, Department of Mechanical Engineering, Belbachir
Belhadj University of Ain Temouchent, 46000 Algeria.

⁴ Laboratoire d'Etude des Structures et de Mécanique des Matériaux, Département de
Génie Civil, Faculté des Sciences et de la Technologie, Université Mustapha Stambouli
B.P. 305, R.P. 29000 Mascara, Algeria.

⁵ Mechanical Systems & Materials Engineering Laboratory,
Mechanical Engineering Department, Faculty of Technology, University of Tlemcen,
BP 230 – 13000, Tlemcen, Algeria.

kebir.tayeb@cuniv-naama.dz

Abstract

In response to the steady rise in global demand for energy resources such as gas and oil, there is a pressing need to enhance the efficiency and safety of pipeline transportation systems. These systems, integral for transferring vast amounts of energy, must operate under increasingly higher pressures and larger diameters without compromising reliability. This study focuses on utilizing finite element analysis (FEA) to investigate the influence of crack orientation and the presence of defects on the fatigue life of pipelines. By simulating internal pressure scenarios and examining various defect characteristics with the AFGROW software, this research applies damage tolerance principles to offer insights into the fatigue behavior of pipelines. The findings can be applied to extend the operational life and ensure the integrity of these critical infrastructures, thereby supporting the sustainable and safe transport of energy resources.

Keywords: pressure equipment, pipelines, fatigue, safety, reliability, loading.

Article category: research article

Introduction

Pressure equipment is widely used in contemporary industry, for example, in the transport and storage of fluids (petroleum, gas, water, and oil). Pipeline transport is the cheapest and safest way to transport large amounts of energy over long distances (Zhang, Sun, et al., 2018). The steady rise in the world's demand for energy resources, such as gas and oil, is propelling the development of new pipelines with optimal profitability, requiring increases in pressures and diameters (Cristoffanini et al., 2014).

Further increasing the resistance of pipelines is becoming a necessity, as is improving their mechanical and chemical characteristics. In certain strategic sectors, such as aeronautics, the automotive industry, or oil infrastructure, fatigue accounts for more than half of the sources of failures observed in real-world systems. The integrity of structures in service crucially depends on their resistance to such fatigue. Under real service conditions, these structures are often subjected to complex and non-proportional cyclic loadings and are not immune to mechanical attacks, giving rise to surface defects that represent favorable sites for the initiation and propagation of cracks (Ballantyne, 2008; Irfan & Omar, 2017).

Pipelines, in particular, are susceptible to various types of defects, such as fatigue cracking, corrosion, etc. (Mohitpour et al, 2010; Zarea et al, 2012). Stress concentrations have been found to account for about 70% of crack initiation and subsequent ruptures in service (European Gas Pipeline Incident Data Group, 2020; Alberta Energy Regulator, 2020). The presence of such defects can be very harmful, and their fatigue behavior becomes dangerously unpredictable, hence the importance of quantifying fatigue damage for the prevention of failures in the oil and gas pipeline industry.

When there is a risk of catastrophic failure, such as bursting at the location of a crack, the concept of damage tolerance becomes a key tool. Broek (1989) defined damage tolerance as the capacity of a structure to withstand damage in the form of cracks without consequences until the damaged component can be repaired. Evaluation of crack propagation rates and prediction of the residual fatigue life are important for the design of structures and their maintenance under the effect of cyclic loading (the fatigue phenomenon). A number of published studies have proposed propagation models for cyclic loadings under constant amplitude and/or variable amplitudes (the phenomenon of overload or underload) (Kocańda & Torzewski, 2009; Jaształ et al., 2010). For aircraft structures, Moussouni et al. (2022) have developed an empirical model based on the Gamma function under applied constant amplitude loading. This model has used experimental data for aluminum alloy 2024 T351 published by Benachour et al. (2017), where best correlation is given comparatively to experimental data and Paris' law.

There are two types of models. Empirical models (Paris & Erdogan, 1963; Elber, 1970), which only constitute an analytical description of results obtained in the laboratory by empirically incorporating the influence of various factors, are therefore limited to the framework that was used to establish them, unlike theoretical models (Forman et al., 1967; Weertman, 1973; Bibly et al., 1963) – the latter, in turn, have the disadvantage of rarely taking into account the role of the various factors. Currently, numerical models are finding application in simulating the behavior of crack propagation across all kinds of investigated materials (Fuiorea et al., 2009; Augustin, 2009; Witek,

2011). Several models have been proposed to predict the growth kinetics of defects, depending not only on the amplitude of the applied load, but also on all the factors affecting their propagation (Kebir et al, 2017; Kebir et al., 2021). The lifetime of these structures has been estimated using several methods.

Moreover, it has also been noted that many metal structures are affected by fatigue corrosion (Kudari & Sharanaprabhu, 2017; Kamińska et al., 2020; Czaban, 2017). Other studies (Sun & Cheng, 2019; Soares et al., 2019; Chen et al., 2015; Hredil et al., 2020) have investigated pipelines with interacting corrosion defects. Fatigue behavior of two interacting 3D cracks in an offshore pipeline has been studied by Low (2021) using FEM. A simulation model to study fatigue behavior was developed by Zhang, Xiao, et al. (2018).

Modern aircraft use different types of pipes to transport fuel, hydraulic fluids, compressed air and other fluids essential to their proper operation. Defects in pipes due to corrosion effects can have significant consequences on aircraft leading to a reduction in their structural strength. This can lead to leaks or even rupture of the pipes, which compromises the safety of the aircraft.

In the present study, the AFGROW calculation code and the NASGROW model describing the crack growth rate are used to predict the fatigue life of pipelines with defects subjected to internal pressure. The influence of several parameters (pipe thickness, defect size, pipe radius and internal pressure) on the lifetime is examined.

1. Finite element analysis of crack direction effects of pipeline

This section examines the behavior of an external crack in the wall of a tube subjected to internal pressure. We are only interested in longitudinal and circumferential tube cracks, as these are important causes of leaks of transported fluid. We also studied the influence of the length of the crack on its propagation using the stress intensity factor; this work is part of the linear mechanics of fracture. In all this we used the Abaqus software, which allowed us to quantify the fracture in materials by the stress intensity factor.

The process simulation includes the geometric configuration of the tube ($L = 1000$ mm, $D = 350$ mm) followed by the tube under boundary conditions of internal pressure ($P = 10$ bars) and the mechanical properties of XC52 steel (Table 1). Also, we chose a finite quadratic type of mesh as appropriate for our case study (Figure 1).

Table 1. Mechanical properties of X52 steel. (Harter, 2002; NASA, 2001)

Young's modulus E (MPa)	200
Poisson's ratio ν	0.30
Yield stress σ_Y (MPa)	410
Ultimate tensile stress σ_{UTS} (MPa)	498
Elongation ϵ_f (%)	35
Toughness fracture (Mpa.mm ^{1/2})	95
Threshold (MPa.mm ^{1/2})	7

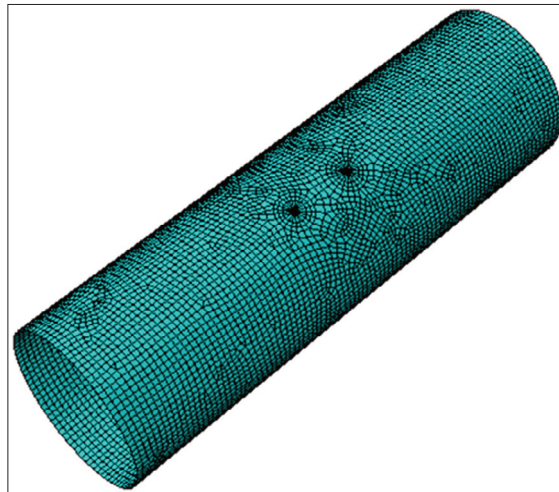


Figure 1. Mesh of the pipe.

Firstly, the simulation consists in seeing the stress distribution S_{yy} at the crack tip for the two cases studied: longitudinal and circumferential cracks in the tube wall. Given the concentration of stresses at the crack tip creating local plastification, the size of this zone must remain small compared to the length of the crack, so as to disrupt the structure of the pipeline, which leads to a fracture (Figure 2).

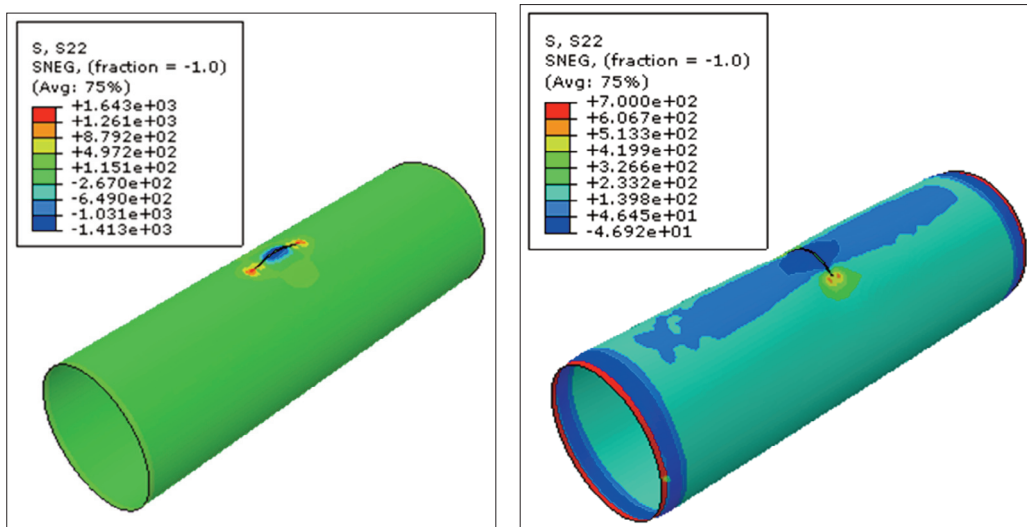


Figure 2. Stress distribution S_{yy} in the case of a) longitudinal (axial) crack, b) circumferential (transversal) crack.

Figure 3 shows the evolution of the integral J as a function of crack length for a longitudinal (axial) crack and circumferential (transversal) crack, respectively. Comparison of the J integral values in Fig. 3 shows that the circumferential crack is more dangerous than the longitudinal crack with respect the cracks size. This change in variable behavior may be explained in terms of changes in the mode of loading. One can deduce that the type loading is responsible for the failure mode of API 5L X52 pipe

in the presence of a defect. The same result has been observed by Benhamena et al. (2011), where the J integral values are found to be more important for a longitudinal crack as compared to a circumferential crack. In other studies, however, the opposite case is reported, with integral J values for a longitudinal pipe crack being significantly greater as compared to those for a circumferential crack (Kaddouri et al., 2004; Mechab et al., 2020).

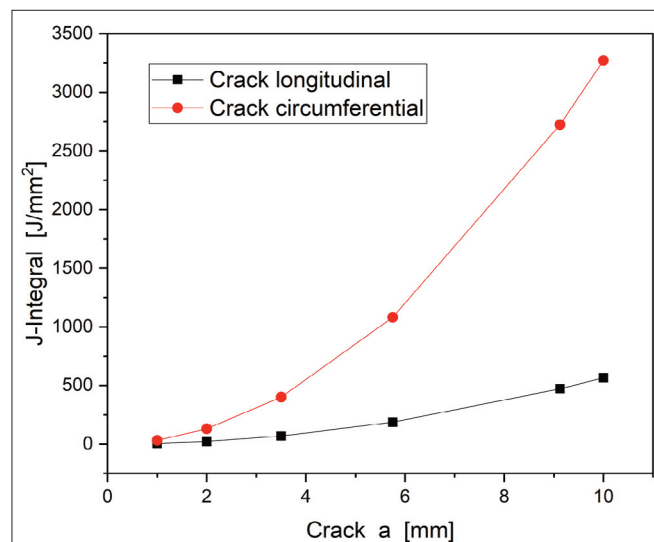


Figure 3. J-integral versus crack length.

Figures 4 and 5, respectively, present the stress intensity factor (SIF) for mode I and II (KI and KII) as function of the crack length for both crack orientations (longitudinal and circumferential). The resulting curves indicate that the SIF is large for a circumferential crack as compared to a longitudinal crack. The difference is important for crack length greater than 3.5 mm in mode I. On the other hand, the SIF for mode II (KII) is largely greater for the circumferential crack.

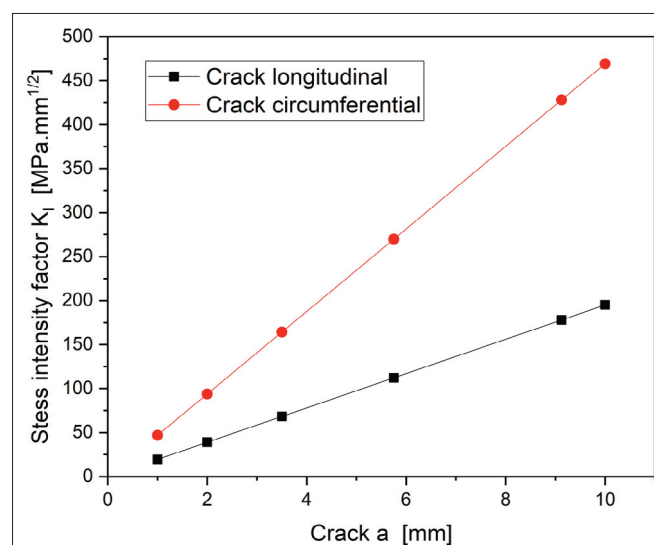


Figure 4. Stress intensity factor K_I versus crack length.

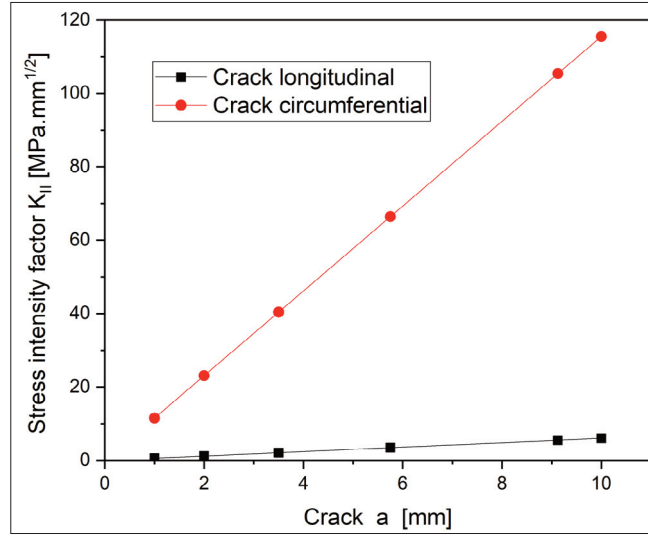


Figure 5. Stress intensity factor K_{II} versus crack length.

2. NASGROW crack growth model

Fatigue life was predicted by a numerical simulation in the AFGROW software (Harter, 2002) using the NASGRO crack growth rate equation (NASA, 2001), given by the relation (1):

$$\frac{da}{dN} = C \left[\left(\frac{1-f}{1-R} \right) \Delta K \right]^n \frac{\left(\frac{\Delta K}{1 - \frac{th}{\Delta K}} \right)^p}{\left(1 - \frac{K_{max}}{K_{crit}} \right)^q} \quad (1)$$

Where K_{max} is the maximum applied stress intensity factor and K_{crit} is the critical stress intensity factor at rupture; N is the number of applied fatigue cycles; a is the crack length; R is the stress ratio; ΔK is the amplitude factor of stress intensity factor; C , n , p , and q are empirically derived constants; and f is Newman's closure function (NASA, 2001), introduced to take into account the phenomenon of fracture closure induced by plasticity:

$$f = \frac{K_{op}}{K_{max}} \begin{cases} \max(R, A_0 + A_1 R + A_2 R^2 + A_3 R^3) \rightarrow \text{with } : R \geq 0 \\ A_0 + A_1 R \rightarrow \text{with } : -2 \leq R \leq 0 \\ A_0 - 2A_1 \rightarrow \text{with } : R \leq -2 \end{cases} \quad (2)$$

Where K_{op} is the stress intensity factor corresponding to the opening load, A_0 , A_1 , A_2 , and A_3 are coefficients such that:

$$A_0 = 0.825 - 0.34\alpha + 0.05\alpha^2 \left[\cos\left(\frac{\pi}{2} S_{\max} / \sigma_0\right) \right]^{1/\alpha} \quad (3)$$

$$A_1 = (0.415 - 0.071\alpha) \cdot S_{\max} / \sigma_0 \quad (4)$$

$$A_2 = 1 - A_0 - A_1 - A_1 - A_1 \quad (5)$$

$$A_3 = 2A_0 + A_1 - 1 \quad (6)$$

σ_0 is plane stress factor; S_{\max}/σ_0 is the ratio of the maximum stress applied to the flow stress; α is the constraint parameter which is used to take into account the stress state effect into account. According to theory, when there is plane stress, the value of α is 1, and when there is plane strain, it is 3.

The threshold stress intensity factor amplitude is given by relation (7):

$$\Delta K_{th} = \Delta K_0 \frac{\left(\frac{a}{a+a_0}\right)^{1/2}}{\left(\frac{1-f}{(1-A_0)(1-R)}\right)^{(1+C_{th}R)}} \quad (7)$$

Where ΔK_0 is the threshold stress intensity factor amplitude for $R = 0$; a is the crack length; a_0 is the initial crack length; C_{th} is the threshold coefficient; R is load ratio.

The algorithm for simulation by the AFGROW calculation code and the model NASGROW to predict fatigue life of a pipeline subjected to internal pressure is shown in Figure 6.

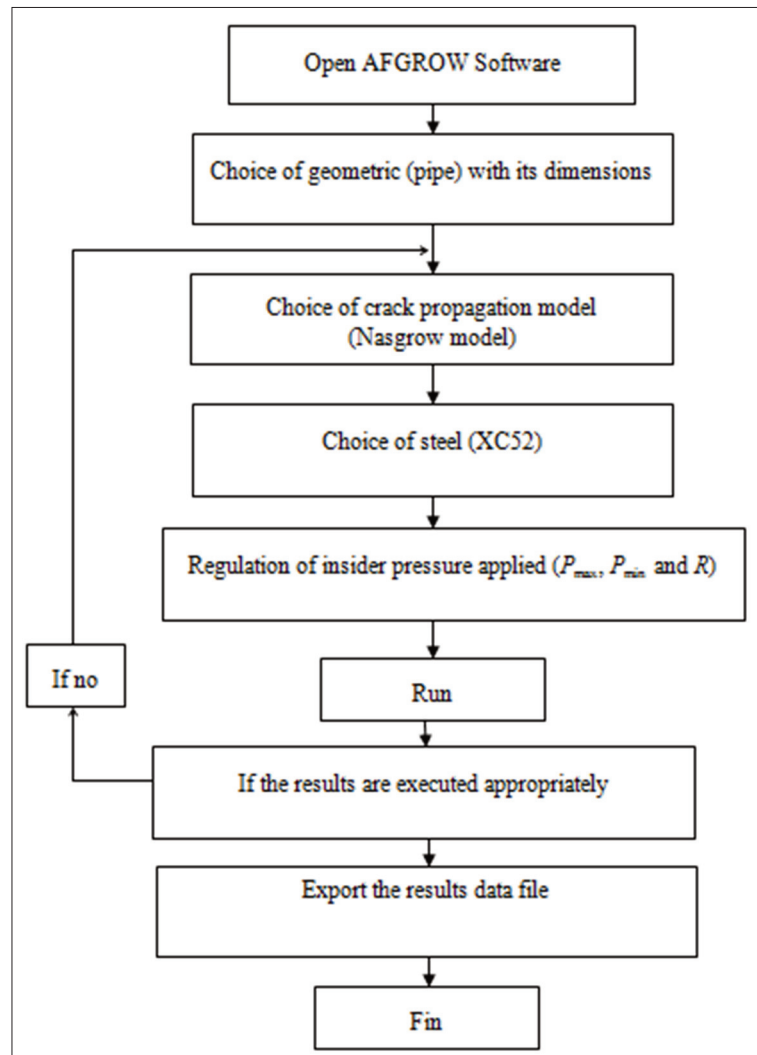


Figure 6. An organogram of fatigue life prediction in AFGROW.

3. Case study

3.1 Material studied

The material used in this study was API 5L Grade B, X52 steel, produced by AMPTA (Arcelor Mittal pipe and Algeria tube). Mechanical properties for the NASGROW model are presented in Table 2. Given the importance of pipeline distances and for good profitability, gas and oil companies use around ten grades of steel in different shades (Grade A, Grade B, X42, X46, X52, X56, X60, X65, X70, X80, etc.) (Harter, 2002; NASA, 2001).

Table 2. Mechanical properties of X52 steel for NASGROW model.
(Harter, 2002; NASA, 2001)

Young's modulus E (MPa)	200
Poisson's ratio ν	0.30
Yield stress σ_Y (MPa)	410
Ultimate tensile stress σ_{UTS} (MPa)	498
Elongation ε_f (%)	35
Toughness fracture K_c (Mpa.mm ^{1/2})	95
Threshold K_{th} (Mpa.mm ^{1/2})	200
p	0.65
q	0.001
C	1.15e-10
n	2.41

3.2 Dimensions and geometry of crack and pipe

In this study we considered, we consider a longitudinal semi-elliptical crack present in the internal wall of the pipe. The geometry of the pipe is shown schematically in Figure 7.

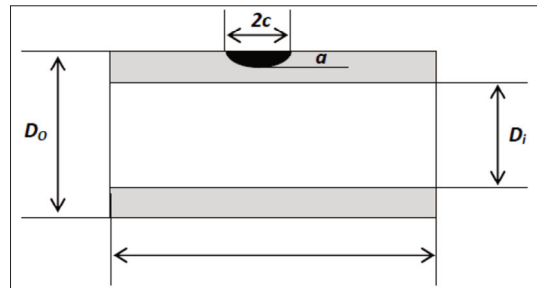


Figure 7. Geometrical parameters of semi-elliptic crack and pipe.

The dimensions of the pipe are as follows: W is the length of the specimen pipe, t is the pipe wall thickness, D_0 the outer diameter and D_i the inside diameter. For all simulations tests, the length is constant and equal to 100 mm.

Semi-elliptical flaws are characterized by the two ratios a/t and a/c , where a is the crack depth and c is the crack length. These reports are: the ratio of the depth crack to the thickness of the cylinder, a/t and the shape parameter defining the elongation of the ellipse or aspect ratio, a/c .

4. Results and discussion

4.1 Influence of the thickness

In this section of this study, four different thicknesses were considered ($t = 1.5, 2.5, 3.5,$ and 5 mm). The specimen was subjected to internal pressure $P = 25$ bars and load ratio $R = 0.1$, with crack depth $a = 1.27$ mm and the length crack $c = 1.27$ mm. The test simulation conditions are shown in Table 3.

Table 3. Test simulation conditions with different values of relative depth a/t .

Test	D_o mm	D_i mm	t mm	a/t
1	350	344	3	0.30
2	350	342	4	0.25
3	350	340	5	0.20
4	350	339	6	0.16

Figures 8 to 11 present the evolution of the crack depth and length crack (a and c) according to the number of cycles N . Note that a crack in the direction of the thickness propagates more quickly than a crack in the lengthwise direction.

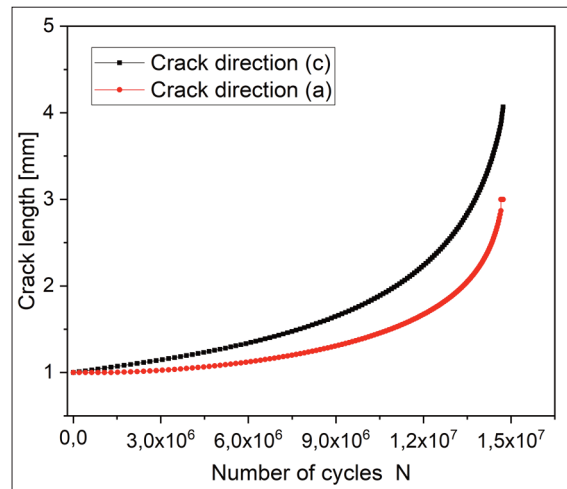


Figure 8. Evolution of the crack depth a and crack length c according to the number of cycles N ($t = 3$ mm).

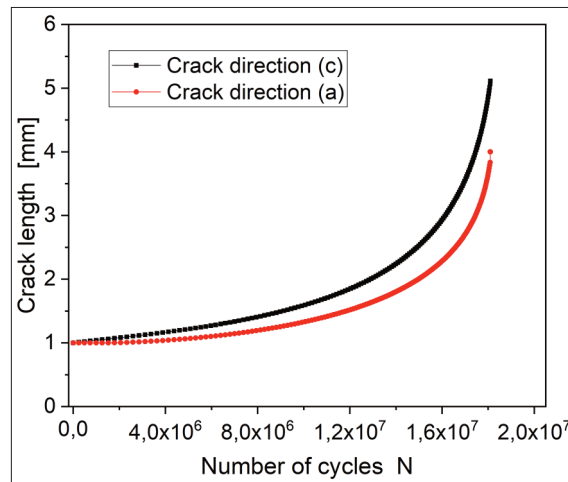


Figure 9. Evolution of the crack depth a and crack length c according to the number of cycles N ($t = 4$ mm).

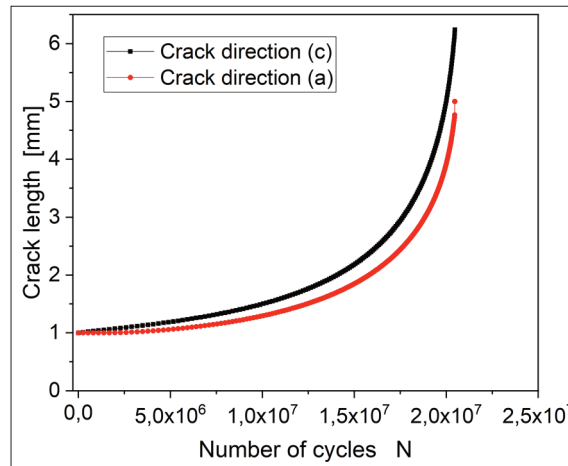


Figure 10. Evolution of the crack depth a and crack length c according to the number of cycles N ($t = 5$ mm).

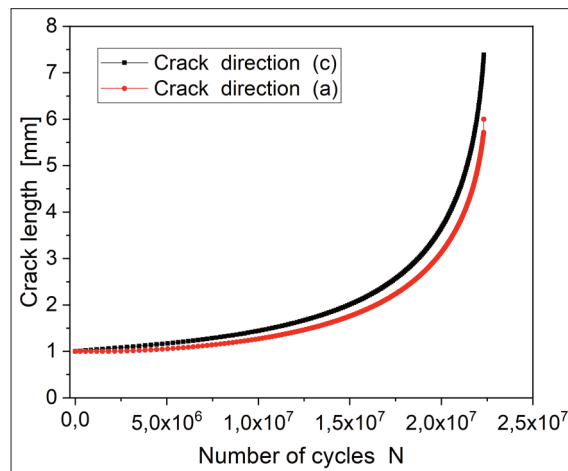


Figure 11. Evolution of the crack depth a and crack length c according to the number of cycles N ($t = 6$ mm).

Figures 12 and 13, respectively, show the evolution of the crack depth and crack with respect to number cycles for different relative crack depth a/t .

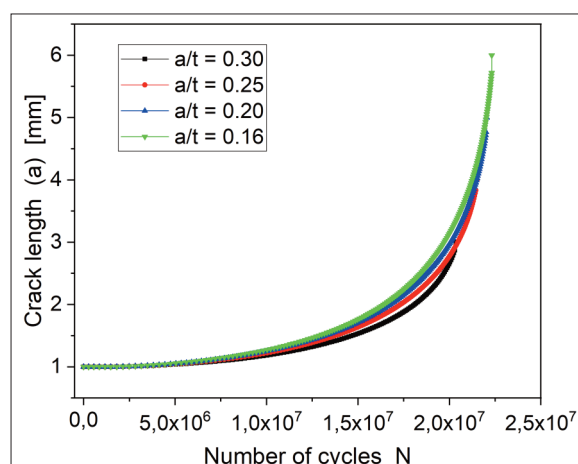


Figure 12. Evolution of the crack length c according to the number of cycles N for different ratios a/t .

Figure 13 shows the evolution of the relative crack depth a/t with respect the number of cycles N . Note when the relative crack depth a/t decreases, the fatigue life increases.

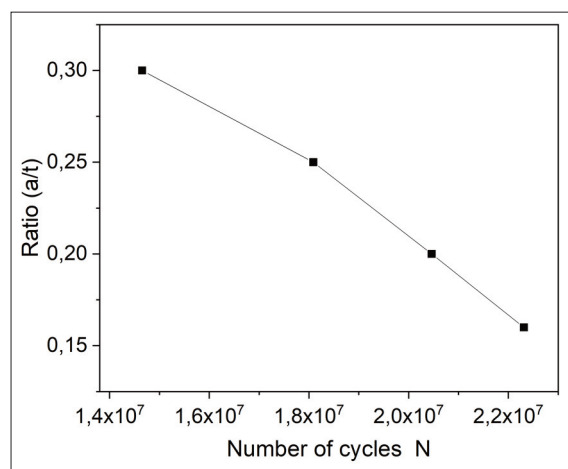


Figure 13. Evolution of the relative crack depth a/t according to the number of cycles N .

4.2 Influence of defect size

In this section of the study, we considered the influence of defect size on fatigue lifetime. Seven aspect ratios (a/c) are studied. The test simulation conditions are presented in Table 4. The pipe is subjected to an internal pressure of 25 bars, and the thickness and length are respectively equal to 5 mm and 100 mm for all tests.

Table 4. Tests simulation conditions with different values of aspect ratio a/c .

Test	Depth	Length	Aspect ratio
	a mm	c mm	a/c
1	1	1	1
2	1	1.2	0.83
3	1	1.4	0.71
4	1	1.6	0.62
5	1	1.8	0.55
6	1	2	0.50

The evolution of the aspect ratio (a/c) as a function of the number of cycles (N) is presented in Figure 14. When the ratio (a/c) increases, the service life increases, this shows that a semicircular crack is more dangerous as compared to a circular crack.

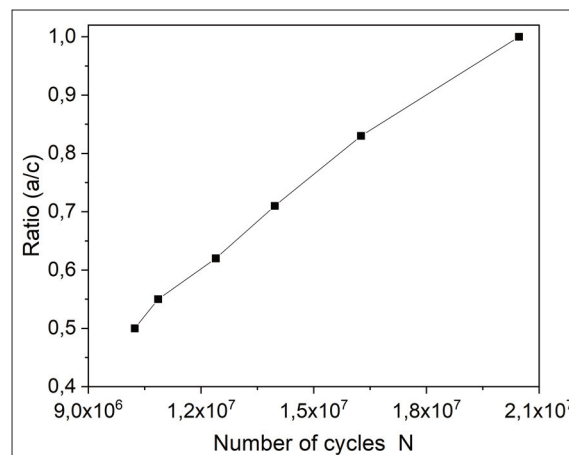


Figure 14. Evolution of the aspect ratio a/c according to the number of cycles N .

4.3 Influence of outer duct diameter

The dimensions of the structure are important parameters; for this purpose, we have simulated several tests by varying the radius of the pipeline. Table 5 presents the dimensions of the pipe and the crack.

Table 5. Tests simulation conditions with different values of outer diameter D_o .

Test	D_o mm	D_i mm	t mm	a/t
1	350	340	5	0.2
2	345	335	5	0.2
3	340	330	5	0.2
4	335	325	5	0.2

Figures 15 to 18 present the evolution of the transversal and longitudinal crack lengths (a and c) according to the number of cycles N respectively for different values of duct diameter outer ($D_o = 350; 345; 340$ and 335 mm). Note that a crack in the direction of the thickness propagates more quickly than a crack in the lengthwise direction.

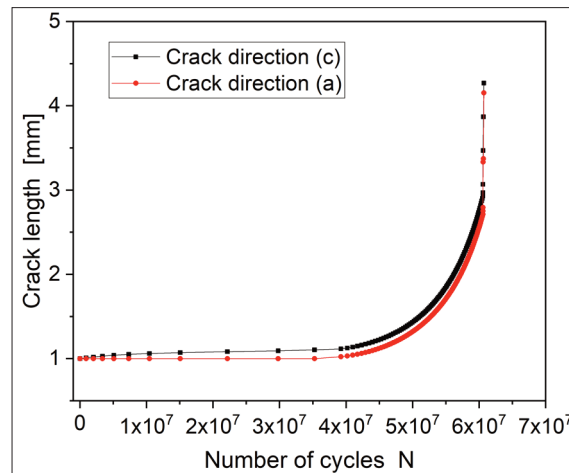


Figure 15. Evolution of the crack depth and length crack (a and c) according to the number of cycles N ($D_o = 350$ mm)

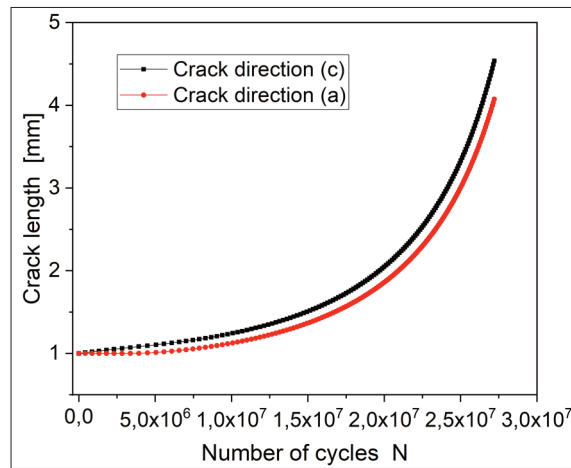


Figure 16. Evolution of the crack depth and length crack (a and c) according to the number of cycles N ($D_o = 345$ mm)

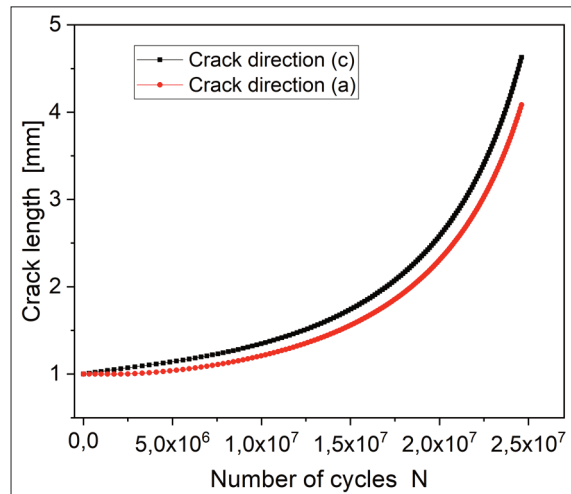


Figure 17. Evolution of the crack depth and length crack (a and c) according to the number of cycles N ($D_o = 340$ mm)

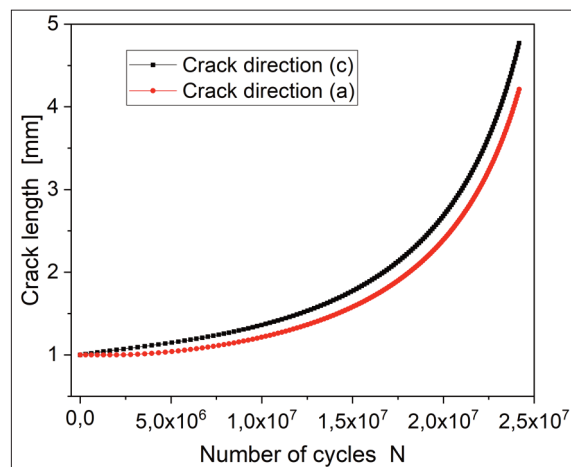


Figure 18. Evolution of the crack depth and length crack (a and c) according to the number of cycles N ($D_o = 335$ mm)

Figure 19 shows the evolution of the outside diameter of the pipe according to the number of cycles. An increase in the outside diameter of the pipe leads to an increase in fatigue life.

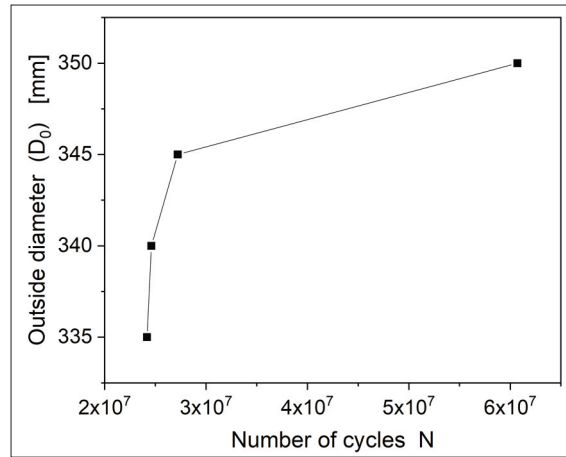


Figure 19. Evolution of outside diameter of pipe D_o as a function of number of cycles N .

4.3 Influence of internal pressure

Four pressure values ($P = 22.5, 24, 25,$ and 26 bars) were considered to study the influence of internal pressure on fatigue life. The geometric parameters considered are internal diameter $D_i = 15$ mm, the thickness $t = 5$ mm, and the width $W = 100$ mm, assuming an initial crack with depth $a = 1.27$ mm and length $c = 1.25$ mm. These parameters were introduced in the AFGROW software.

Figure 20 shows the evolution of the depth of transversal crack and length of longitudinal crack respect to number cycles for different values of internal pressure. Note that an increase in internal pressure leads to an increase in the crack propagation rate and, consequently, to a reduction in the fatigue life.

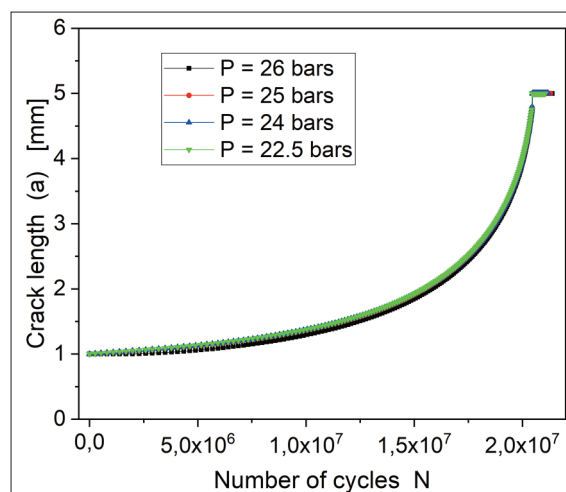


Figure 20. Evolution of the crack depth and length (a and c) according to the number of cycles N for different values of internal pressure.

The evolution of internal pressure with respect to number cycles is presented in Figure 21. As this figure shows, high internal pressure leads to short fatigue life and when the pressure decreases, the fatigue life increases.

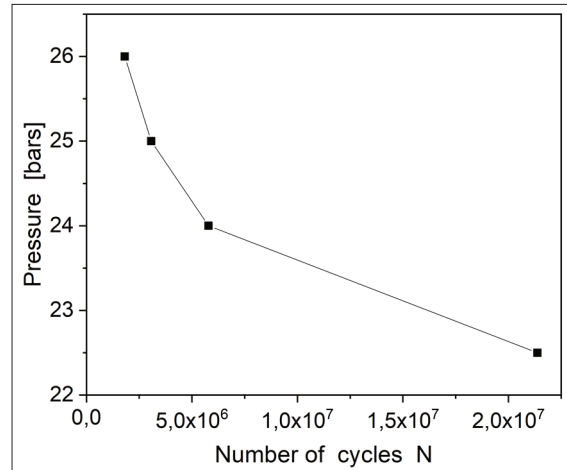


Figure 21. Internal pressure versus number of cycles N .

5. Conclusions

This comprehensive numerical study has produced several critical findings regarding the fatigue life of pipelines in the face of defects and crack orientations.

- Most notably, it establishes that circumferential (transversal) cracks pose a higher risk than their longitudinal (axial) counterparts, due to differences in loading modes.
- Additionally, it was discovered that cracks oriented perpendicular to the pipe's length tend to propagate more rapidly.
- The study also highlights the greater danger presented by semi-circular cracks over circular ones, emphasizes the beneficial impact of increasing pipe section on resistance to loading, and reveals that a larger conduit radius enhances the service life.
- A crucial observation is the inverse relationship between applied pressure and service life, underlining the need for careful pressure management to prevent premature pipeline failure.

Overall, the findings of this research may help improve the maintenance and monitoring strategies used for fluid transport systems, particularly in the aviation sector, by providing a deeper understanding of crack evolution in pipelines. Through the application of finite element analysis, this work not only aids in predicting the fatigue life of pipelines more accurately but also facilitates informed decision-making regarding their integrity and maintenance.

Acknowledgment

This work was carried out in the Laboratory of Materials and Reactive Systems of Djillali Liabes University of Sidi Bel Abbes, which is sponsored by the Directorate-General for Scientific Research and Technological Development (DGRST Algeria).

References

- Alberta Energy Regulator. (2020). *Pipeline Performance* (New Reports). <https://www.aer.ca/protecting-what-matters/holding-industry-accountable/industry-performance/pipeline-performance>
- Augustin, P. (2009). Simulation of fatigue crack growth in integrally stiffened panels under the constant amplitude and spectrum loadin. *Fatigue of Aircraft Structures*, 2009(1), 5–19. <https://doi.org/10.2478/v10164-010-0001-2>
- Ballantyne, D. (2008). *M7.8 Southern San Andreas Fault Earthquake Scenario: Oil and Gas Pipelines* (California Geological Survey Preliminary Report 25 version 1.0). MMI Engineering.
- Benachour, M., Benachour, N., & Benguediab, M. (2017). Fractographic observations and effect of stress ratio on fatigue striations spacing in aluminium alloy 2024 T351. *Materials Science Forum*, 887, 3–8. <https://doi.org/10.4028/www.scientific.net/msf.887.3>
- Benhamena, A., Aminallah, L., Bouiadjra, B. B., Benguediab, M., Amrouche, A., & Benseddiq, N. (2011). J integral solution for semi-elliptical surface crack in high density poly-ethylene pipe under bending. *Materials & Design*, 32(5), 2561–2569. <https://doi.org/10.1016/j.matdes.2011.01.045>
- Bibby, B. A., Cotrell, A. H., & Swinden, K. H. (1963). The spread of plastic yield from a notch. *Proceedings of the Royal Society of London. Series A. Mathematical and Physical Sciences*, 272(1350), 304–314. <https://doi.org/10.1098/rspa.1963.0055>
- Broek, D. (1989). *The practical use of fracture mechanics*. Kluwer Academic Publishers. <https://doi.org/10.1002/mawe.19890200504>
- Chen, Y., Zhang, H., Zhang, J., Liu, X., Li, X., & Zhou, J. (2015). Failure assessment of X80 pipeline with interacting corrosion defects. *Engineering Failure Analysis*, 47, 67–76. <https://doi.org/10.1016/j.engfailanal.2014.09.013>
- Cristoffanini, C., Karkare, M., & Aceituno, M. (2014). Transient simulation of long-distance tailings and concentrate pipelines for operator training. *Presented at SME Annual Meeting/Exhibit, February 24-26, 2014, Salt Lake City, UT, USA*, 1–7. <https://www.andritz.com/resource/blob/15062/50bf8f04c35997dbce9c51b8b3d2fab3/aa-dynamic-simulation-long-tailings-concentrate-pipelines-data.pdf>
- Czaban, M. (2018). Aircraft corrosion – review of corrosion processes and its effects in selected cases. *Fatigue of Aircraft Structures*, 2018(10), 5–20. <https://doi.org/10.2478/fas-2018-0001>
- Elber, W. (1970). Fatigue crack closure under cyclic tension. *Engineering Fracture Mechanics*, 2, 445–476.

European Gas Pipeline Incident Data Group. (2020). *Gas Pipeline Incidents: 11th Report of the European Gas Pipeline Incident Data Group (period 1970 – 2019)* (Doc. number VA 20.0432). <https://www.egig.eu/reports>

Fatigue crack growth computer program 'NASGRO' version 3.0 – reference manual (Technical Report JSC-22267B). (2001). NASA. <http://www.nasgro.swri.org>

Forman, R. G., Kearney, V. E., & Engle, R. M. (1967). Numerical analysis of crack propagation in cyclic-loaded structures. *Journal of Basic Engineering*, 89(3), 459–463. <https://doi.org/10.1115/1.3609637>

Fuiorea, I., Bartis, D., Nedelcu, R., & Frunzulica, F. (2009). Numerical models for fatigue crack evolution study. *Fatigue of Aircraft Structures*, 2009(1), 42–49. <https://doi.org/10.2478/v10164-010-0004-z>

Harter, J. A. (2002). *AFGROW users guide and technical manual*. (Technical Report AFRL-VA-WP-TR-2002-XXX). U.S. Air Force Research Laboratory. <http://afgrow.wpafb.af.mil>

Hredil, M., Krechkovska, H., Tsyurulnyk, O., & Student, O. (2020). Fatigue crack growth in operated gas pipeline steels. *Procedia Structural Integrity*, 26, 409–416. <https://doi.org/10.1016/j.prostr.2020.06.052>

Irfan, O. M., & Omar, H. M. (2017). Experimental study and prediction of erosion-corrosion of AA6066 aluminum using artificial neural network. *Engineering, Materials Science*, 17(06), 17–31. <https://www.ijens.org/IJMMEVol17Issue06.html>

Jasztal, M., Kocanda, D., & Tomaszek, H. (2010). Predicting fatigue crack growth and fatigue life under variable amplitude loading. *Fatigue of Aircraft Structures*, 2010(2), 37–51. <https://doi.org/10.2478/v10164-010-0024-8>

Kaddouri, K., BachirBouaidjra, B., Belhouari, M., & Madani, K. (2004). Elastic plastic analysis of cracks in pipe. In *15th European Conference on Fracture: ECF 15 - advanced fracture mechanics for life and safety assessments: Aug.11 - 13, 2004, KTH Stockholm, Sweden*.

Kamińska, P., Synaszko, P., Ciężak, P., & Dragan, K. (2020). Analysis of the corrosion resistance of aircraft structure joints with double-sided rivets and single-sided rivets. *Fatigue of Aircraft Structures*, 2020(12), 57–68. <https://doi.org/10.2478/fas-2020-0006>

Kebir, T., Benguediab, M., & Imad, A. (2017). A model for fatigue crack growth in the paris regime under the variability of cyclic hardening and elastic properties. *Fatigue of Aircraft Structures*, 2017(9), 117–135. <https://doi.org/10.1515/fas-2017-0010>

Kebir, T., Correia, J. A. F. O., Benguediab, M., & Imad, A. (2021). A FCG model and the graphical user interface under Matlab for predicting fatigue life: Parametric studies. *Fatigue of Aircraft Structures*, 2021(13), 116–139. <https://doi.org/10.2478/fas-2021-0011>

- Kocańda, D., & Torzewski, J. (2009). Deterministic approach to predicting the fatigue crack growth in the 2024-T3 aluminum alloy under variable amplitude loading. *Fatigue of Aircraft Structures*, 2009(1), 102–115. <https://doi.org/10.2478/v10164-010-0010-1>
- Kudari, S. K., & Sharanaprabhu, C. M. (2017). The effect of anodizing process parameters on the fatigue life of 2024-t-351-aluminium alloy. *Fatigue of Aircraft Structures*, 2017(9), 109–115. <https://doi.org/10.1515/fas-2017-0009>
- Low, E. T. (2021). *FEM fatigue simulation for an offshore pipeline containing interacting cracks* (Final Year Project (FYP)). Nanyang Technological University. <https://hdl.handle.net/10356/148866>
- Mechab, B., Malika, M., Salem, M., & Boualem, S. (2020). Probabilistic elastic-plastic fracture mechanics analysis of propagation of cracks in pipes under internal pressure. *Frattura ed Integrità Strutturale*, 14(54), 202–210. <https://doi.org/10.3221/igf-esis.54.15>
- Mohitpour, M., Murray, A., McManus, M., & Colquhoun, I. (2010). *Pipeline Integrity Assurance*. ASME Press. <https://doi.org/10.1115/1.859568>
- Moussouni, A., Benachour, M., & Benachour, N. (2023). Prediction of fatigue cracks using gamma function. *Fatigue of Aircraft Structures*. <https://doi.org/10.2478/fas-2022-0004>
- Paris, P. C., & Erdogan, F. (1963). A critical analysis of crack propagation laws. *Journal of Basic Engineering*, 85, 528–533.
- Soares, E., Bruère, V. M., Afonso, S. M. B., Willmersdorf, R. B., Lyra, P. R. M., & Bouchonneau, N. (2019). Structural integrity analysis of pipelines with interacting corrosion defects by multiphysics modeling. *Engineering Failure Analysis*, 97, 91–102. <https://doi.org/10.1016/j.engfailanal.2019.01.009>
- Sun, J., & Cheng, Y. F. (2019). Modelling of mechano-electrochemical interaction of multiple longitudinally aligned corrosion defects on oil/gas pipelines. *Engineering Structures*, 190, 9–19. <https://doi.org/10.1016/j.engstruct.2019.04.010>
- Weertman, J. (1973). Theory of fatigue crack growth based on a BCS Crack theory with work hardening. *International Journal of Fracture*, 9, 125–131. <https://doi.org/10.1007/BF00041854>
- Witek, L. (2011). Experimental and numerical crack initiation analysis of the compressor blades working in resonance conditions. *Fatigue of Aircraft Structures*, 2011(3), 134–153. <https://doi.org/10.2478/v10164-010-0045-3>
- Zarea, M., Piazza, M., Vignal, G., Jones, C., Rau, J., & Wang, R. (2013). Review of R&D in support of mechanical damage threat management in onshore transmission pipeline operations. *Proceedings of the 2012 9th International Pipeline Conference. Volume 2: Pipeline Integrity Management*. Calgary, Alberta, Canada. September 24–28, 2012. ASME, 569–582.

Zhang, C., Sun, X., Li, Y., Zhang, X., Zhang, X., Yang, X., & Li, F. (2018). Hydraulic characteristics of transporting a piped carriage in a horizontal pipe based on the bidirectional fluid-structure interaction. *Mathematical Problems in Engineering*, 2018, 1–27. <https://doi.org/10.1155/2018/8317843>

Zhang, Y., Xiao, Z., & Luo, J. (2018). Fatigue crack growth investigation on offshore pipelines with three-dimensional interacting cracks. *Geoscience Frontiers*, 9(6), 1689–1697. <https://doi.org/10.1016/j.gsf.2017.09.011>